ER Stress Is Involved in T17M Rhodopsin-Induced Retinal Degeneration

Mansi M. Kunte,[1] *Shreyasi Choudhury,*[1] *Jessica F. Manheim,*[1] *Vishal M. Shinde,*[1] *Masayuki Miura,*[2] *Vince A. Chiodo,*[3] *William W. Hauswirth,*[3] *Oleg S. Gorbatyuk,*[4] *and Marina S. Gorbatyuk*[†,1]

Purpose. The human rhodopsin (*Rho*) mutation T17M leads to autosomal dominant retinitis pigmentosa (adRP). The goal of our study was to elucidate the role of endoplasmic reticulum (ER) stress in retinal degeneration in hT17M *Rho* mice and identify potential candidates for adRP gene therapy.

Methods. We used transgenic mice expressing the ER stress-activated indicator (ERAI) and hT17M *Rho* to evaluate the activation of ER stress responses. Quantitative reverse transcription PCR (qRT-PCR) was used to analyze changes in the expression of 30 unfolded protein response (UPR)-associated genes at P12, 15, 18, 21, and 25. The cytosolic fraction of hT17M *Rho* retinal cells was used to measure the release of cytochrome *C* and apoptotic inducing factor-1 (AIF1) by Western blotting. Optical coherence tomography (OCT) analysis was performed for 1-month-old hT17M *Rho* mice.

Results. hT17M *Rho* was localized in the outer nuclear layer (ONL) of $T17M^{+/-}ERAI^{+/-}$ photoreceptors as well as C57BL/6 retinas injected with AAV-hT17M Rho-GFP. In P15 hT17M Rho retinas, we observed an up-regulation of UPR genes (*Atf4, Eif2α, Xbp1, Bip, Canx,* and *Hsp90*), autophagy genes and proapoptotic Bcl2 genes. OCT, and the downregulation of *Nrl* and *Crx* gene expression confirmed that cell death occurs in 55% of photoreceptors via the up-regulation of caspase-3 and caspase-12, and the release of AIF1 from the mitochondria.

Conclusions. The ER stress response is involved in retinal degeneration in hT17M *Rho* mice. The final demise of photoreceptors occurs via apoptosis involving ER stress-associated and mitochondria-induced caspase activation. We identified *Atg*5, *Atg*7, *Bax*, *Bid*, *Bik,* and *Noxa* as potential therapeutic targets for adRP treatment. (*Invest Ophthalmol Vis Sci.* 2012;53:3792–3800) DOI:10.1167/iovs.11-9235

From the [1]Department of Cell Biology and Anatomy, University of North Texas Health Science Center. Fort Worth, Texas; [2]Laboratory of Cell Recovery Mechanisms, Brain Science Institute, Wako, Saitama, Japan; and the Departments of [3]Ophthalmology and [4]Molecular Genetics and Microbiology, University of Florida, Gainesville, Florida.

Supported by National Institutes of Health Grant R01EY020905, Foundation Fighting Blindness Grant TA-GT-0409-0508-NTERI, a Hope for Vision grant, and DOD Grant W81XH-10-2-0003.

Submitted for publication December 3, 2011; revised April 26, 2012; accepted April 30, 2012.

Disclosure: **M.M. Kunte**, None; **S. Choudhury**, None; **J.F. Manheim**, None; **V.M. Shinde**, None; **M. Miura**, None; **V.A. Chiodo**, None; **W.W. Hauswirth**, None; **O.S. Gorbatyuk**, None; **M.S. Gorbatyuk**, None

Current affiliation: Masayuki Miura, Department of Genetics, Graduate School of Pharmaceutical Sciences, The University of Tokyo and CREST, JST, Tokyo, Japan.

Corresponding author: Marina S. Gorbatyuk, Department of Cell Biology and Anatomy, North Texas Eye Research Institute, UNTHSC, 3500 Camp Bowie Blvd., Fort Worth, TX 76107; marina.gorbatyuk@unthsc.edu.

Mutations in the *rhodopsin* gene (*Rho*) were the first genetic components to be implicated in autosomal dominant retinitis pigmentosa (adRP).[1] T17M rhodopsin is an example of a class II mutant opsin with a defect in protein folding.[2] The substitution of threonine to methionine at position 17 occurs so close to the N2–N15 glycosylation site that it presumably affects the folding of the protein.[3] Previous in vitro studies have shown that bovine T17M *Rho* partially reconstitutes with 11-*cis*-retinal and is transported to the cell membrane,[4] whereas human T17M *Rho* preferably accumulates in the endoplasmic reticulum (ER), and binds poorly to the chromophore.[5] In contrast, in vivo studies in *Xenopus laevis* have shown that glycosylation is not crucial for rhodopsin biosynthesis or trafficking.[3] Recently, a difference between the in vitro and in vivo expression of N-terminally truncated fragments of human wild-type *Rho* has been examined carefully.[6] The truncated *Rho* has been shown to remain in the ER in vitro, whereas it can be trafficked to the rod outer segments (ROS) in vivo. Therefore, an analysis of prior studies allows us to conclude that T17M mutant rhodopsin behaves differently in vitro and in vivo, and can abolish the N-terminal glycosylation site and relocate to the ROS. To find the exact mechanism by which the human T17M mutant causes the disease, it is important to monitor the progression of adRP in a system that mimics the human disease closely, such as in hT17M *Rho* transgenic mice. In addition, if our study shows that a mutant protein remains in the ER, the next step would be to examine the activity of the unfolded protein response (UPR) or ER stress response in hT17M *Rho* retinas.

ER stress initiates three transduction pathways, the PERK, ATF6, and IRE signaling pathways, which can confer protective and pro-apoptotic effects during ER stress.[7] Recently, the UPR has attracted growing attention from researchers investigating the mechanism underlying retinitis pigmentosa (RP) in animal models.[8–10] Moreover, it has become clear that the response to ER stress can be modulated therapeutically at three major levels: 1) upstream of ER stress sensors, by decreasing the amount of misfolded rhodopsin, 2) at the level of ER stress sensors, by attenuating their activation, and 3) downstream of ER stress transducers, by modulating the interaction network responsible for the implementation of ER stress.[11] In hT17M *Rho* retinas, the role of the UPR has not been studied to our knowledge. Therefore, we are interested in elucidating the role of ER stress responses in the death of hT17M *Rho* photoreceptors to validate new therapeutic targets for adRP treatment. We analyzed transgenic retinas to determine whether the

hT17M mutant triggers the UPR and whether the activation of the UPR promotes ER-stress-associated apoptosis. In our study, we determined the localization of a mutant form of rhodopsin in vivo, directly monitored ER stress in vivo using ER stress-activated indicator (ERAI) transgenic mice,[12] and established a dynamic link between ER stress and the activation of other pro- and anti-apoptotic pathways. To our knowledge, our study is the first comprehensive analysis of the cellular pathways involved in the pathogenesis of hT17M *Rho* photoreceptors that identifies future targets for adRP gene therapy.

Materials and Methods

Animals

Transgenic mice expressing human T17M *Rho*, C57BL/6 mice, and ERAI mice were used for this study. The animal protocol was approved by the University of North Texas Health Center Animal Care and Use Committee, and was conducted following animal guidelines according to the ARVO statement for the Use of Animals in Ophthalmic and Vision Research. All animals were reared with 12-hour day and night cycles at a light intensity of less than 10 lux, as measured with a light meter (model 401036; Extech, Waltham, MA), since the light exposure is known to affect retinal function and morphology of hT17M *Rho* mice.[13] To demonstrate that the hT17M transgene caused the ER stress, we crossed $T17M^{+/-}$ mice with $ERAI^{+/-}$ mice expressing an XBP1-GFP fusion gene (purchased from Riken Co., Tokyo, Japan). Eyes from F1 progeny with the genotypes $T17M^{+/-}$ $ERAI^{+/-}$ $T17M^{-/-}$ $ERAI^{+/-}$, and CB57L6 were inoculated and fixed as described previously.[14] GFP expression was detected using direct fluorescence or immunohistochemistry in 12 μm cryostat retina sections. As a positive control, 1 μL of a 2 mg/mL tunicamycin solution was injected subretinally into $T17M^{-/-}$ $ERAI^{+/-}$ mice. Eyes were collected 24 hours after injection for further analysis.

Mouse tails were collected, and the DNA was extracted using a 2.0× Taq RED Master Mix Kit (Apex, San Diego, CA). To identify the $T17M^{+/-}$ genotype, PCR was performed with human rhodopsin-specific primers (sense: 5′-GAGTGCACCCTCCTTAGGCA-3′ and anti-sense: 5′-TCCTGACTCGAGGACCCTAC-3′). The presence of a single band of ~300 base pairs (bp) signified a positive result. To identify the $ERAI^{+/-}$ genotype, PCR was performed using four primers (primer 1, 5′-GAACC AGGAGTTAAGACAGC-3′; primer 2, 5′-GAACAGCTCCTCGCCCTTGC-3′; primer 3, 5′-CTAGGCCACAGAATTGAAAGATCT-3′, and primer 4, 5′-CATGGTGGAAATTCTAGCATCATCC-3′). Primers 1 and 2 amplified a 240 bp fragment indicating the presence of the fusion transgene. Primers 3 and 4 provided an internal control and amplified a 324 bp fragment. The presence of two bands indicated a positive result.

Whole retinas were collected from individual $T17M^{+/-}$ (referred to as hT17M *Rho* mice from here on) and wild-type sibling pups at postnatal (P) days 12, 15, 18, 21, and 25. RNA was extracted using RNeasy mini prep kits (Qiagen, Valencia, CA). After treating the RNA with DNaseI (Invitrogen, Grand Island, NY), it was converted to cDNA using Super Script II Reverse Transcriptase (Invitrogen).

Quantitative Reverse Transcription PCR (qRT-PCR)

We used a custom Taqman array plate with 32 genes, including *Gapdh* as endogenous controls (Applied Biosystems, Carlsbad, CA). qRT-PCR was performed using ~50 ng of cDNA mixed with TaqMan universal PCR master mix (Applied Biosystems) and the StepOnePlus Real-Time PCR system (Applied Biosystems, $N = 4$ for each time point). The fold changes were calculated by dividing the mean of the relative quantities (RQs) for the hT17M *Rho* mice by the mean RQ of the wild-type mice at each time point.

Immunostaining

Immunostaining of cryostat sections of retinas was performed as described[15] using anti-GFP (Abcam, Cambridge, MA) and anti-rhodopsin 1D4 antibodies (University of British Columbia, Vancouver, BC, Canada). Cy-5- and Cy-2-conjugated secondary antibodies (Jackson ImmunoResearch Laboratories, Inc., West Grove, PA) were used to identify the localization of the GFP and rhodopsin proteins. Propidium iodide (Vector Laboratories, Inc., Burlingame, CA) was used to stain the nuclei of the retina cells. Images of the retinas were obtained using confocal microscopy.

Isolation of Cytoplasmic Fractions from hT17M *Rho* Retinas and Western Blot Analysis

The cytosolic fractions of three individual retinas from wild-type and transgenic mice were isolated using the Mitochondria Isolation Kit for Tissues (Thermo Scientific, Inc., Rockford, IL) and the Dounce stroke method, as recommended by the manufacturer. The protein concentration of each fraction was measured using a Biorad protein assay, and 40 μg of total protein were loaded on 12% SDS-PAGE gel (Biorad, Hercules, CA). Specific antibodies were used to detect cytochrome C (Santa-Cruz Biotechnology Inc., Santa Cruz, CA) and apoptotic inducing factor-1 (AIF1; Santa-Cruz Biotechnology Inc.). The membrane then was stripped, and β-actin (Sigma-Aldrich, St. Louis, MO) was detected as an internal control. The protein detection was performed using an infrared secondary antibody and an Odyssey infrared imager (Li-Cor Biosciences Inc., Lincoln, NE). The absence of mitochondrial contamination in the cytoplasmic fractions was confirmed by Western blot using an anti-Cox IV antibody (Abcam).

Additionally, Western blotting was performed to detect the UPR markers. Total protein was isolated from wild-type and transgenic retinas, and protein concentration was measured as above. Specific antibodies were used to detect Bip (Santa-Cruz Biotechnology Inc.), CHOP (Abcam), ATF6 (Imgenex Corp., San Diego, CA), and pEif2α (Cell Signaling Technology, Danvers, MA). The membrane then was stripped and β-actin was detected as internal control.

Optical Coherence Tomography (OCT) Analysis

At 1 month of age, hT17M *Rho* mice and their wild-type ($T17M^{-/-}$) siblings ($N = 4$) were anesthetized with intraperitoneal injections of 50 mg/kg ketamine and 50 mg/kg xylazine. Each mouse's pupils were dilated with 2.5% phenylephrine hydrochloride, and Systane Ultra was applied to both eyes after a few minutes. We measured the thickness of the outer nuclear layer (ONL) of the retina using the Bioptigen Spectral Domain Ophthalmic Imaging System (SDOIS) (Durham, NC). Six calibrated calipers were placed in the superior and inferior hemispheres of the retina within distances of 100, 200, 300, and 400 μm from the optic nerve head.

Statistical Analysis

Two-way ANOVA (GraphPad Software, Inc., La Jolla, CA) was used to analyze the RQs obtained from the qRT-PCR and OCT data. A *t*-test was used to analyze a normalized protein content in retinal protein extracts of hT17M *Rho* and wild-type mice. A P value higher than 0.05 was considered significant.

Results

ER Stress Was Activated in hT17M *Rho* Transgenic Mice

ERAI mice carry *venus*, a variant of green fluorescent protein fused with a partial sequence of human *Xbp1* that includes the 26 nucleotide (nt) ER-stress-specific intron.[12] Under stress conditions, the *Xbp1-venus* fusion mRNA undergoes alternative splicing to remove the 26 nt intron, which puts *venus* in frame and results in the expression of green fluorescent protein (GFP). In our experiment, we observed green

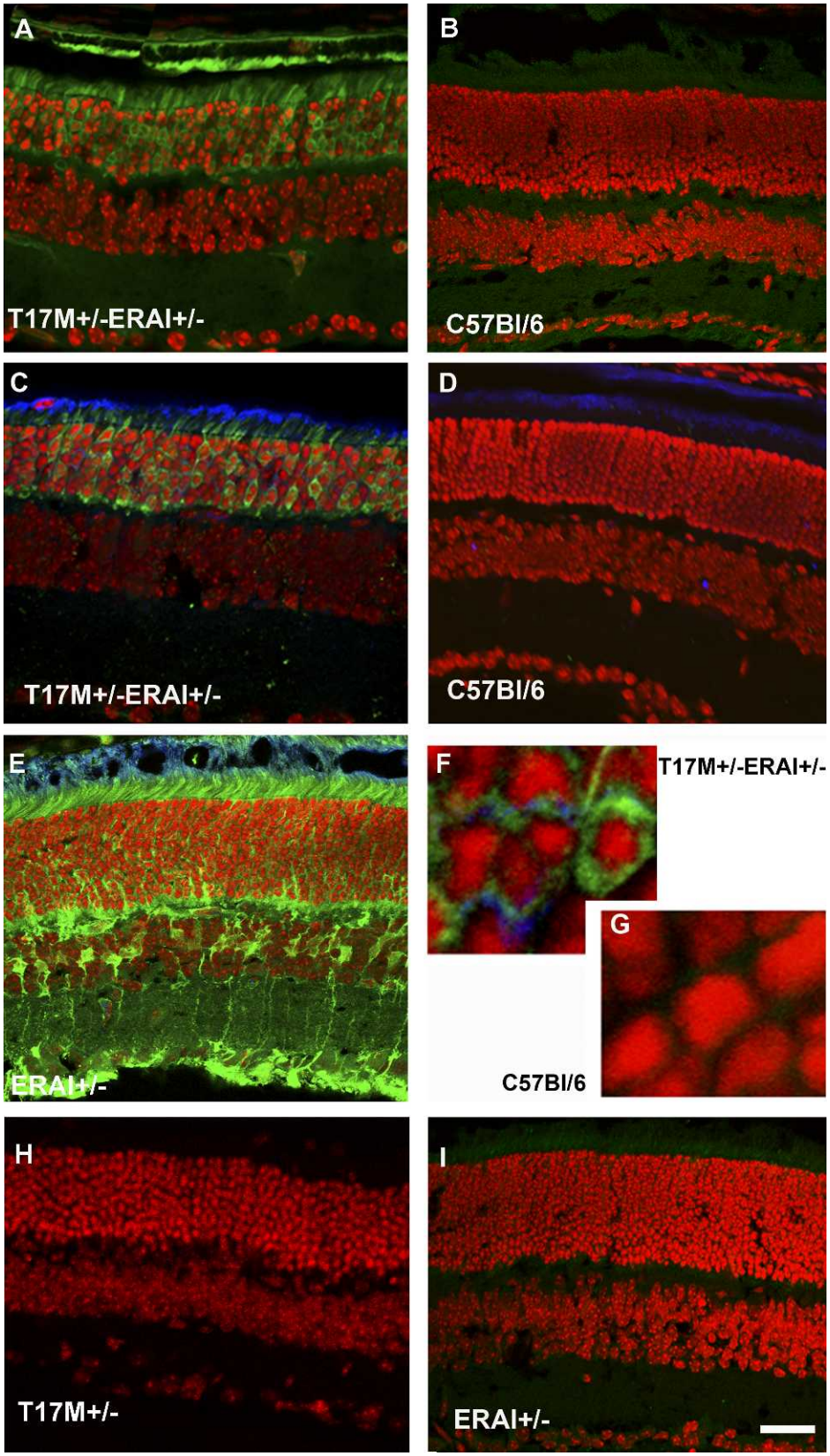

Figure 1. hT17M rhodopsin leads to activation of the ER stress response at P15 in T17M$^{+/-}$ ERAI$^{+/-}$ mice. Confocal microscopy is used to obtain images of mouse retinas. Propidium iodide is used to stain the nuclei (*red*). GFP protein expression (*green*) results from the splicing of the Xbp1-GFP transcription factor (detected by direct fluorescence or immunohistochemical analysis). For immunohistochemistry, an anti-GFP antibody is used to stain the sXbp1-GFP. The primary anti-rhodopsin antibody 1D4 and secondary anti-mouse Cy5-conjugated antibodies are applied to detect the localization of rhodopsin (*blue*). T17M$^{+/-}$ ERAI$^{+/-}$ (**A**) and C57BL/6 (**B**) images of retinas are obtained via direct observation under a fluorescence microscope. T17M$^{+/-}$ ERAI$^{+/-}$ (**C**), C57BL/6 (**D**), ERAI$^{+/-}$ positive control with tunicamycin injection (**E**), T17M$^{+/-}$ ERAI$^{+/-}$ (**F**), and

C57BL/6 (**G**) images of retinas are obtained after immunostaining with anti-GFP and anti-rhodopsin antibodies. GFP fluorescence is observed in images T17M$^{+/-}$ ERAI$^{+/-}$ (**A**), T17M$^{+/-}$ ERAI$^{+/-}$ (**C**), ERAI$^{+/-}$ positive control with tunicamycin injection (**E**), and T17M$^{+/-}$ ERAI$^{+/-}$(**F**), and not in the negative controls C57BL/6 (**B**), C57BL/6 (**D**), C57BL/6 (**G**), T17M$^{+/-}$ (**H**), and ERAI$^{+/-}$ (**I**). Accumulation of rhodopsin is observed in T17M$^{+/-}$ ERAI$^{+/-}$ (**F**) but is not detected in C57BL/6 (**G**). Scale bar indicates 30 μm (**A–E**, **H**, **I**) and 300 μm (**F**, **G**).

fluorescence in the ONL of T17M$^{+/-}$ ERAI$^{+/-}$ photoreceptors (Fig. 1) at P15, suggesting that the ER stress response is activated by this time point and that the mutant hT17M *Rho* causes ER stress. No fluorescence was observed in the ERAI$^{+/-}$ and T17 M$^{+/-}$ retinas.

Next, we injected subretinally ERAI$^{+/-}$ retinas with a solution of tunicamycin (ER stress inducer) 24 hours before performing immunohistochemical analysis and observed fluorescence in the injected retinas. This confirmed that the fluorescent signal detected in T17M$^{+/-}$ ERAI$^{+/-}$ retinas was a result of an activated ER stress response. In T17M$^{+/-}$ ERAI$^{+/-}$ retinas, we also found that rhodopsin was retained partially within the ER. Similar localization was observed in C57BL/6 retinas injected with AAV5-hT17M Rho-GFP (Supplementary Fig. S1, http://www.iovs.org/lookup/suppl/doi:10.1167/iovs.11-9235/-/DCSupplemental).

Genes Involved in UPR Were Up-Regulated in hT17M *Rho* Retinas

The first UPR gene to show up-regulation was *Bip* at P15. *Bip* is a molecular chaperone that recognizes misfolded proteins. Its expression was increased ~ 1.5-fold compared to the wild-type (control) at P15 ($P < 0.0001$, Fig. 2, Supplementary Table S1, http://www.iovs.org/lookup/suppl/doi:10.1167/iovs.11-9235/-/DCSupplemental). However, at P18 and P21, no significant difference in *Bip* expression was observed. *Bip* expression was elevated significantly again at P25 (an increase of 1.5-fold compared to the control, $P < 0.01$). Other chaperones, such as *Calnexin* (*Cnx*) and *Hsp90B1,* also showed increased expression (Fig. 2, Supplementary Table S1, http://www.iovs.org/lookup/suppl/doi:10.1167/iovs.11-9235/-/DCSupplemental). Expression of *Cnx* was increased in hT17M *Rho* mice 1.3-, 1.3-, 1.6-, and 1.8-fold at P15, P18, P21, and P25, respectively ($P < 0.01$, $P < 0.05$, $P < 0.0001$, and $P < 0.0001$, respectively). Conversely, *Hsp90B1* was not significantly up-regulated after P15 (1.4-fold increase, $P < 0.01$). The *Eif2α* gene also was significantly up-regulated at P15 and P18 (~1.2- and ~1.3-fold increase, $P < 0.05$ and $P < 0.01$, respectively). *Atf4* gene expression, another marker of the PERK pathway that is translated preferentially by phosphorylated Eif2α, was elevated significantly at P15, P18, and P21 (~1.4-fold increase, $P < 0.05$ for all time points) and then declined with time. Interestingly, *CHOP,* which is a target of the ATF4 transcription factor, already was over-expressed at P12 (~1.3-fold increase, $P < 0.01$). Its expression at P15 was increased 1.5-fold ($P < 0.001$). At this time point, expression of the *Eif2α* and *Atf4* genes (PERK pathway) already was elevated. *Atf6* gene expression (ATF6 pathway) was modulated at all time points; however, it was not significantly different from that in the control. *Xbp1* gene expression (IRE1 pathway) was increased significantly from P15 (1.5-fold increase, $P < 0.0001$) until P25.

We verified further the activation of UPR by detecting the UPR markers, like Bip (~1.13-fold increase, $P < 0.05$), pEif2α (~1.24-fold increase, $P < 0.05$), and apoptotic inducer CHOP (~1.14-fold increase, $P < 0.05$) in hT17M *Rho* mice at P15 by Western blot analysis (Fig. 3). As observed at mRNA level, no significant difference in ATF6 protein expression was observed.

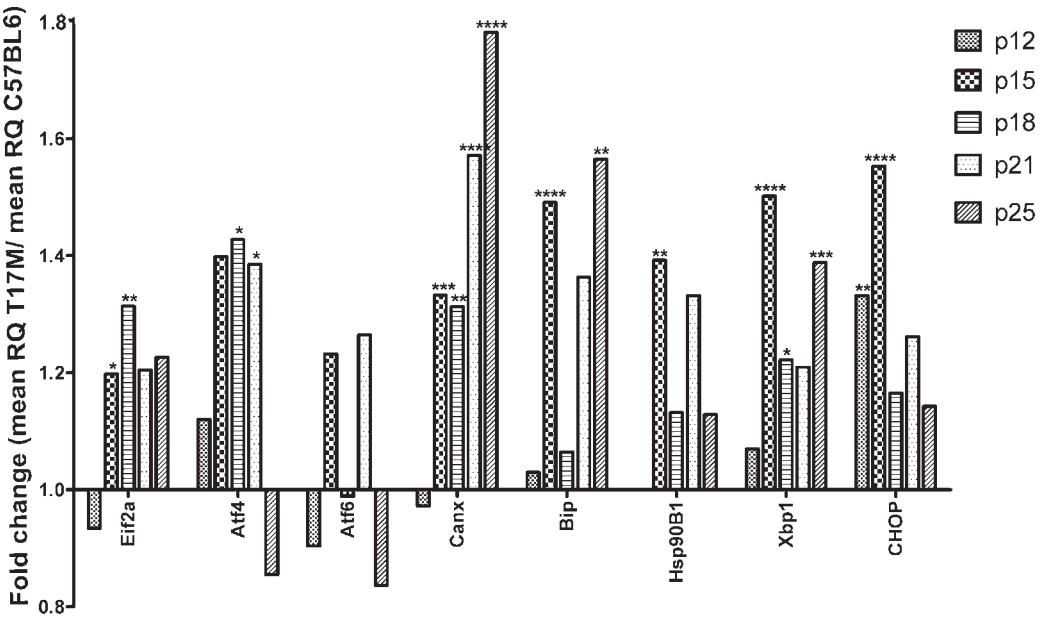

Figure 2. UPR genes are up-regulated at P15. Wild-type gene expression is normalized to 1, and the ratio of hT17M *Rho* to the wild-type is shown. Induction of the expression of the molecular chaperones *BiP, Cnx*, and *Hsp90* in hT17M *Rho* retinas was observed at P15; the observed increases were 1.4-, 1.3-, and 1.4-fold compared to the control. Markers of the PERK (*eiF2a* and *ATF4*) and IRE (*Xbp1*) pathways are up-regulated strongly (1.2-, 1.4-, 1.5-fold increases) at P15, whereas the expression of the *CHOP* gene is up-regulated earlier at P12 (1.3-fold; $^{*}P < 0.05$, $^{**}P < 0.01$, $^{***}P < 0.001$, and $^{****}P < 0.0001$).

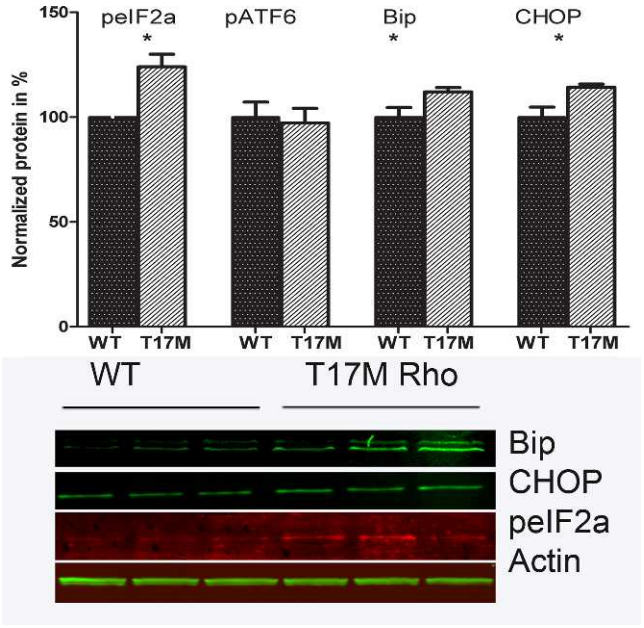

Figure 3. Activation of UPR in hT17M *Rho* retina. The UPR (peIF2α, Bip and Chop) markers were elevated in P15 hT17M *Rho* retina by 1.24-fold (100% ± 4.84% in wild-type vs. 124% ± 5.98% in hT17M *Rho*, $P = 0.048$), by 1.13-fold (100% ± 4.66% in wild-type vs. 113% ± 2.11% in hT17M *Rho*, $P = 0.032$), and by 1.14-fold (100% ± 4.89% in wild-type vs. 114% ± 1.48% in hT17M *Rho*, $P = 0.042$), correspondingly. The pATF6 (50kD) protein is not elevated in hT17M *Rho* retina, suggesting that the ATF6 signaling does not have a prominent role in the pathogenesis of hT17M *Rho* photoreceptors.

Modulation in Mouse and Human *Rho* Gene Expressions in hT17M *Rho* Retina

We analyzed mouse and human *Rho* gene expression in P12, P21, and P30 transgenic retinas, and found that during the adRP progression relative expression of the mouse *Rho* gene declined in time while expression of the human *Rho* gene was elevated steadily (Fig. 4, Supplementary Table S2, http://www.iovs.org/lookup/suppl/doi:10.1167/iovs.11-9235/-/DCSupplemental). Mouse *Rho* expression in hT17M *Rho* retina compared to that in wild-type retina was lowered from 0.83 at P12 to 0.38 at P30 (Supplementary Table S2, http://www.iovs.org/lookup/suppl/doi:10.1167/iovs.11-9235/-/DCSupplemental).

To estimate total Rho protein expression, we performed Western blot analysis and discovered that the "monomer" and "dimer" forms of Rho protein were reduced in P15 transgenic retinas by 28% ($P = 0.014$ and $P = 0.009$, respectively).

Autophagy and Akt Pathway Gene Expressions were Induced in hT17M *Rho* Retinas

In hT17M *Rho* retinas, we detected modulations in expression levels of the autophagy-associated genes (Supplementary Fig. S3, http://www.iovs.org/lookup/suppl/doi:10.1167/iovs.11-9235/-/DCSupplemental) and Akt pathway genes (Supplementary Fig. S4, http://www.iovs.org/lookup/suppl/doi:10.1167/iovs.11-9235/-/DCSupplemental) during the adRP progression.

Modulation of Bcl2-Family Gene Expression in hT17M *Rho* Retinas

The pro-apoptotic members of the *Bcl2* family, *Bax*, *Bid*, and *Bik*, were overexpressed in hT17M *Rho* retinas (Fig. 5, Supplementary Table S1, http://www.iovs.org/lookup/suppl/doi:10.1167/iovs.11-9235/-/DCSupplemental). Their expression was increased significantly by 1.2- to 2.5-fold compared to the control. The *Bim* and *Noxa* genes, however, were overexpressed significantly only at P18 and P21. *Bim* gene expression was up-regulated at P21 by 1.4-fold ($P < 0.001$), and *Noxa* gene expression was increased significantly by 1.5- and 1.8-fold at P18 and P21, respectively ($P < 0.05$ and $P < 0.001$).

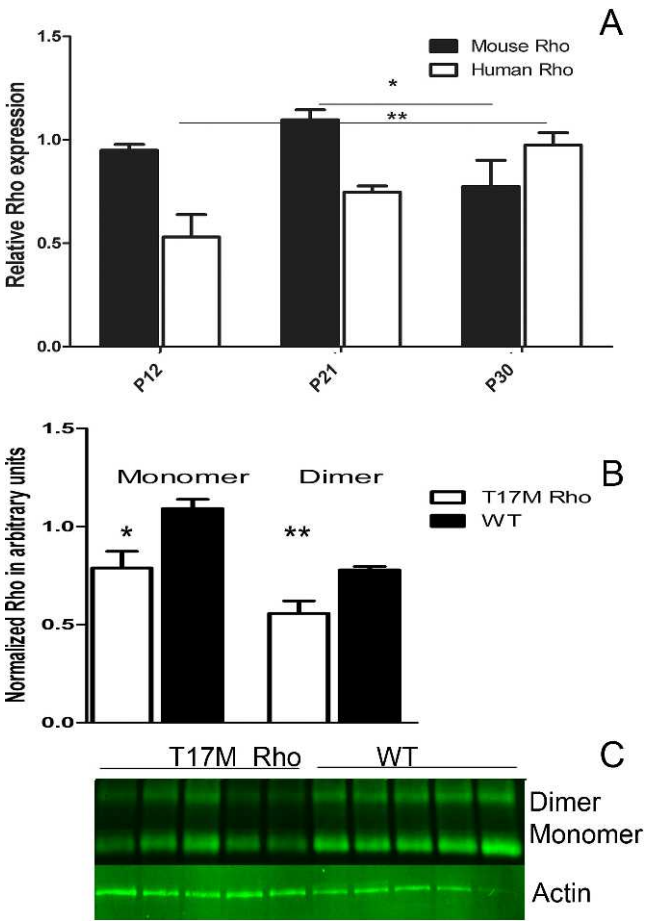

Figure 4. *Rho* gene expression in hT17M *Rho* retina. **(A)** Mouse and human *Rho* gene expression in P12, P21, and P30 hT17M *Rho* retina. Mouse gene expression declines in time from P21 to P30 by 30% (from 1.12 to 0.87, Supplementary Table S2, http://www.iovs.org/lookup/suppl/doi:10.1167/iovs.11-9235/-/DCSupplemental), while human *Rho* gene expression is elevated steadily from P12 to P30 by 83% (from 1.21 to 2.22, Supplementary Table S2, http://www.iovs.org/lookup/suppl/doi:10.1167/iovs.11-9235/-/DCSupplemental). **(B)** Modulation in mouse and human *Rho* expressions leads to reduction in Rho protein level by 28%. **(C)** Image of Western blot treated with anti-Rho antibody.

The anti-apoptotic gene *Bcl2* also was increased by 1.3- to 1.9-fold at all time points from P15 until P25 in hT17M *Rho* retinas except at P18.

Mitochondria-Initiated Apoptosis was Activated in hT17M *Rho* Retinas

Mitochondrial membrane integrity is crucial for cell survival, and mitochondrial outer membrane permeabilization (MOMP) is fatal for the cell. Members of the Bcl-2 family of proteins, such as Bax and Noxa, are known to induce MOMP. Therefore, we decided to isolate the cytoplasmic portion of hT17M *Rho* retinal cells from the mitochondria to analyze the presence of

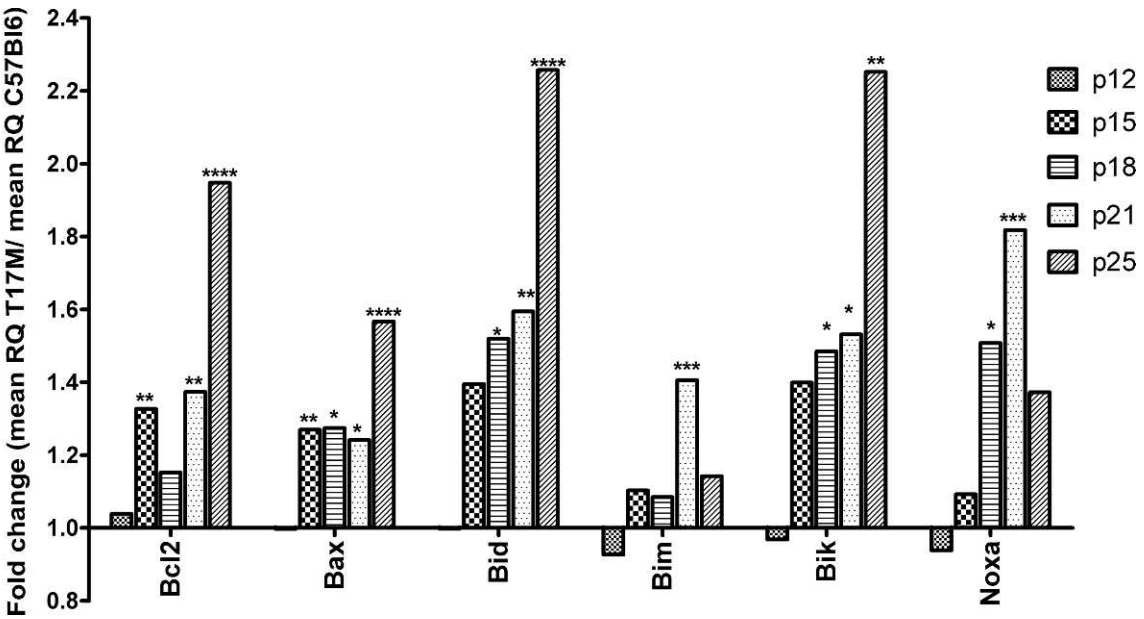

Figure 5. Anti-apoptotic and pro-apoptotic members of the *Bcl2* gene family are up-regulated at P15. Wild-type gene expression is normalized to 1, and the ratio of hT17M *Rho* to the wild-type is shown. The BH3-only proteins Bax, Bid, Bim, Bik, and Noxa are up-regulated in hT17M *Rho* retinas starting from P15. *Bax, Bid,* and *Bik* gene expression is up-regulated continuously over time. At P18, the expression of these genes is increased 1.3-, 1.5-, and 1.5-fold; at P21, the expression of these genes is increased 1.2-, 1.6-, and 1.5-fold; and at P25, the expression of these genes is increased 1.5-, 2.2-, and 2.2-fold, *Bim* and *Noxa* expression, however, declined over time. Surprisingly, expression of the anti-apoptotic *Bcl2* gene also is increased at P15 and remained elevated steadily at subsequent time points. At P15, P18, P21, and P25 its expression is increased 1.3-, 1.1-, 1.3-, and 1.9-fold, respectively. ($^{*}P < 0.05$, $^{**}P < 0.01$, $^{***}P < 0.001$, and $^{****}P < 0.0001$).

the AIF1 and cytochrome *C* proteins. Cytochrome *C* release from the mitochondria was not detected in hT17M *Rho* retinas, while AIF1 protein was present at significant levels (Fig. 6).

hT17M *Rho* Photoreceptors Died via Apoptosis

The executioner *Casp3* also showed a $\sim$ 1.4-fold increase at P15 ($P < 0.01$), and it remained up-regulated (Fig. 7A, Supplementary Table S1, http://www.iovs.org/lookup/suppl/doi:10.1167/iovs.11-9235/-/DCSupplemental). In addition, *Casp12*, which encodes the ER-resident caspase, was induced by 2.5-fold later in the ER stress cycle at P25 ($P < 0.0001$). We observed consistently a downregulation in the expression of *Nrl,* which is a transcriptional regulator of rod-specific genes. Starting from P15, its expression was reduced continuously by 42%, 67%, 45%, and almost 93% ($P < 0.05$, $P < 0.01$, $P > 0.05$, and $P < 0.001$, respectively, Fig. 7B, Supplementary Table S1, http://www.iovs.org/lookup/suppl/doi:10.1167/iovs.11-9235/-/DCSupplemental) Similarly, *Crx,* which also is a photoreceptor-specific transcriptional factor, showed lower expression at P18 (38% reduction, $P < 0.001$) and P25 (62% reduction, $P < 0.0001$). We also examined the thickness of the outer nuclear layer in retinas from 1-month-old hT17M *Rho* mice and their wild-type siblings using OCT. The results of the OCT analysis demonstrated a reduction of approximately 50% ($P < 0.0001$) in the length of the ONL in hT17M *Rho* mice (Fig. 7C).

Discussion

The hT17M *Rho* transgenic mouse model is a very useful tool for understanding the activation of ER stress in adRP. T17M mutant rhodopsin has been described previously in cell lines and *X. laevis*, and to our knowledge this is the first time it has been studied in a mammalian model. We confirm that the mutant hT17M *Rho* induces ER stress in the T17M$^{+/-}$ ERAI$^{+/-}$ mice at P15 due to its retention within the ER or mislocalization to the cytoplasm (Fig. 1). Further study using specialized microscopic techniques will be required to determine whether the mutant protein forms agglomerates in the cytoplasm of hT17M *Rho* cells.

Consistent with our immunohistological analysis of T17M$^{+/-}$ ERAI$^{+/-}$ retinas demonstrating the splicing of the Xbp1 mRNA and activation of the IRE pathway, we found that several genes involved in UPR are over-expressed at P15 in hT17M *Rho* transgenic retinas. Results of the protein analysis also confirm the activation of the UPR in transgenic retina. For example, the PERK signaling is activated in P15 hT17M *Rho* retina. However, the ATF6 pathway is not modified.

It is important to note here that the hT17M *Rho* mouse model has an extra copy of *Rho*. To confirm that this induction of UPR genes was not due to *Rho* overdose but rather the mutant human transgene, we analyzed the hT17M *Rho* mice carrying one copy of mouse *Rho* gene (T17M$^{+/-}$ Rho$^{+/-}$), which were not available for us at the time of the original experiment. Interestingly, these mice demonstrated the same level of modulation of the UPR-associated gene expression compared to hT17M *Rho* (Supplementary Fig. S2, Supplementary Table S3. http://www.iovs.org/lookup/suppl/doi:10.1167/iovs.11-9235/-/DCSupplemental). In T17M$^{+/-}$ Rho$^{+/-}$ mice, we observed up-regulation of the UPR genes along with elevated Bcl2 family and apoptotic genes expression as early as P15 (Supplementary Fig. S2, http://www.iovs.org/lookup/suppl/doi:10.1167/iovs.11-9235/-/DCSupplemental).

Elevation of UPR-associated gene expression also was observed in wild-type retinas injected subretinally with AAV5-hT17M Rho-GFP when compared to AAV5-hRho-GFP injections (Supplementary Fig. S1, Supplementary Table S4, http://www.iovs.org/lookup/suppl/doi:10.1167/iovs.11-9235/-/DCSupplemental). To support our model further, we checked expression of h*Rho* (transgene) and m*Rho* (endogenous *Rho*) in T17M *Rho* and C57BL/6 retinas at P12, P21, and P30 (Fig. 4). Surprisingly, we observed that when the m*Rho* expression

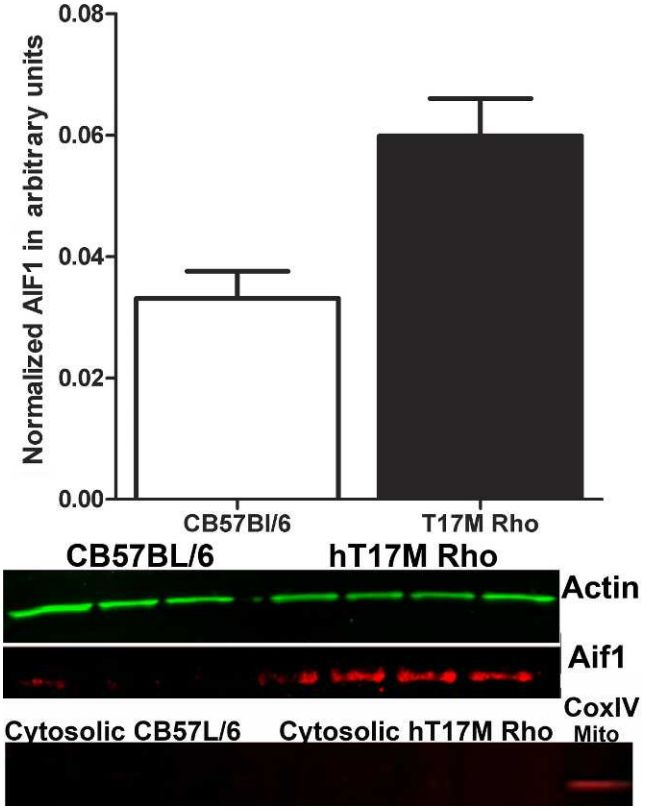

FIGURE 6. Release of AIF1 from the mitochondria of hT17M *Rho* retinas. We isolated the cytosolic fraction of the hT17M *Rho* retinas and performed Western blot analysis to detect AIF1; β-actin is detected as an internal control. A 55% increase in the level of AIF1 was observed in hT17M *Rho* mice. The upper panel shows the results of the quantitative analysis of the intensities of the bands corresponding to AIF1 and β-actin, using the AIF1:β-actin ratio to measure the level of the AIF1 in the cytoplasm. The bottom panel shows images of blots stained for AIF1, β-actin, and the COXIV protein, which was used as a mitochondrial positive control.

declines, the h*Rho* expression increases suggesting a compensatory effect. The total Rho protein in hT17M *Rho*, however, was lower compared to wild-type at P15 (Fig. 4) indicating that the hT17M *Rho* photoreceptors do not over-produce Rho protein.

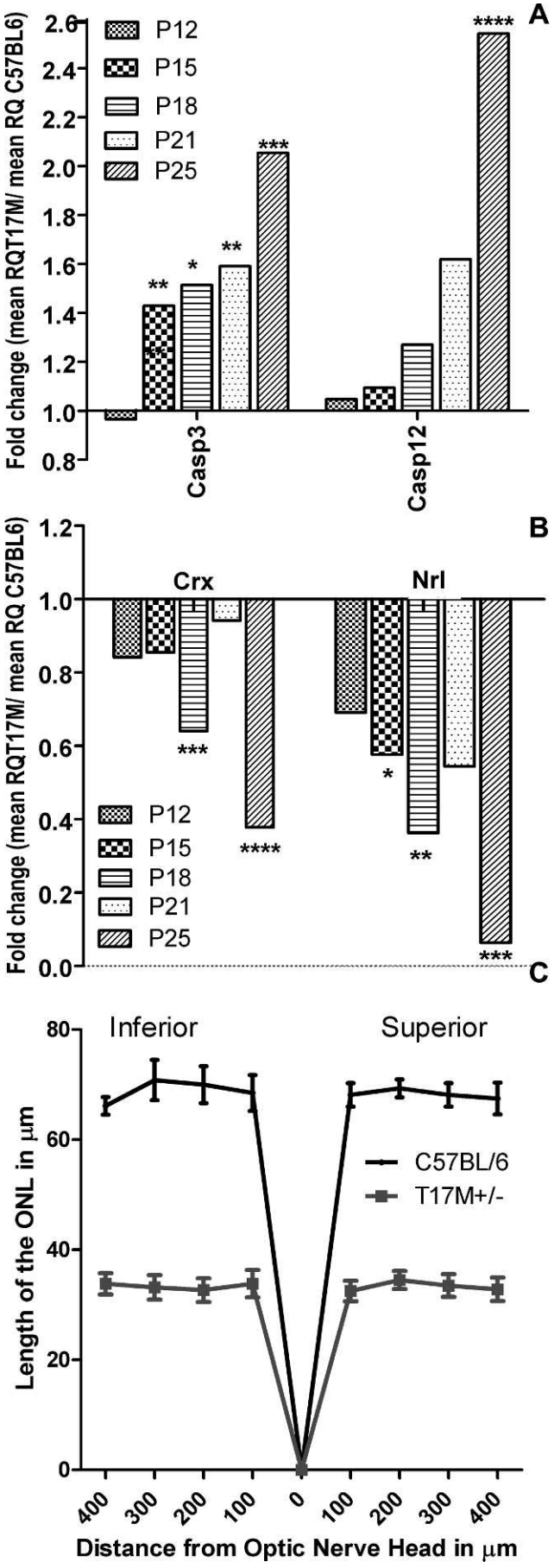

Figure 7. hT17M *Rho* photoreceptor cell death occurs via caspase-dependent apoptosis. (**A**) Caspase-12 (ER-associated) and caspase-3 (executioner) gene expression is up-regulated in hT17M *Rho* retinas. Caspase-3 expression already was increased at P15 (1.4-fold increase) and remained up-regulated until P25 (2-fold increase), while caspase-12 is up-regulated significantly only at P25 (2.5-fold increase), suggesting that ER-stress-induced apoptotic signaling is not the only cause of retinal degeneration in hT17M *Rho* retinas. (**B**) Reductions in the rod-specific genes *Nrl* and *Crx* is observed at P15 and P18, respectively. Wild-type gene expression is normalized to 1, and the ratio of hT17M *Rho* to the wild-type is shown. *Nrl* gene expression is downregulated by 42%, 67%, and 93% at P15, P18, and P25, respectively. *Crx* gene expression is decreased by 38% and 62% at P18 and P25, respectively. The reduction in the expression of photoreceptor-specific genes suggests that degeneration of the hT17M *Rho* photoreceptors starts as early as P15. (**C**) Early apoptosis in T17M *Rho* retinas results in photoreceptor damage in the inferior and superior hemispheres. A 50% ($n = 6$, $P < 0.0001$ for all time points) reduction in the thickness of the ONL is observed in the inferior and superior hemispheres. The graph shows the average ± SEM. ($^{*}P < 0.05$, $^{**}P < 0.01$, $^{***}P < 0.001$, and $^{****}P < 0.0001$).

In hT17M *Rho*, increases in the expression of the molecular chaperones *Bip*, *Cnx*, and *Hsp901B*, suggesting that the hT17M *Rho* ER is overloaded with misfolded proteins, and this overload leads to the activation of ER stress responses (Fig. 2). Markers of the PERK and IRE1 pathways are up-regulated in hT17M *Rho* retinas. For example, expression of the *eIf2α* and *Atf4* genes increases starting at P15. However, the downstream marker, *Chop* gene, is up-regulated significantly by P12, earlier then the expression of its upstream regulators. The basal level of peIf2α protein appears to be sufficient to stimulate the transcription of the nuclear factor ATF4. Even a slight up-regulation of ATF4 at P12 is sufficient to induce the expression of the *Chop* gene. The IRE1 pathway also is up-regulated in hT17M *Rho* retinas by P12. However, it is induced only significantly at P15, which correlates with our immunohistochemical data on splicing of the Xbp1 mRNA (Fig. 1). The ATF6 pathway does not show any specific trend and does not appear to have a significant role in hT17M *Rho* degeneration (Fig. 3). Therefore, our immunohistochemical, gene expression, and Western blot analyses suggest that ER stress is activated in hT17M *Rho* retinas.

An analysis of ERAD gene expression shows no significant changes compared to the control (Supplementary Table S1, http://www.iovs.org/lookup/suppl/doi:10.1167/iovs.11-9235/-/DCSupplemental). However, the autophagy degradation pathway is up-regulated in hT17M *Rho* retinas starting at P15 (Supplementary Fig. S3, http://www.iovs.org/lookup/suppl/doi:10.1167/iovs.11-9235/-/DCSupplemental). This up-regulation appears to be connected to the over-expression of the UPR and *Atf4* genes that has been shown to induce autophagy.[16] At this point, it is not clear whether autophagy exerts a pro-survival effect in hT17M *Rho* retinas by degrading mutant agglomerates or promotes a pro-death, non-apoptotic form of programmed cell death involving the bulk degradation of the cytoplasmic contents. Additional experiments to analyze hT17M *Rho* retinas lacking the *Atg5* or *Atg7* genes will be necessary to answer this question.

BH3-only proteins are regarded as the initial responders to incoming stress signals.[17] In our experiments, we observed the overexpression of *Bax*, *Bid*, *Bim*, *Bik*, and *Noxa* during ER stress, which suggests that pro-apoptotic stimuli are induced in hT17M *Rho* photoreceptors. Over-expression of BH3-only genes appears to be related to p53 activation in hT17M *Rho* retinas. A link between ER stress and the activation of p53 has been proposed recently.[18] *Bax* and *Bik* also have been shown to be regulated translationally by p53,[19,20] and the release of Bid proteins from Bcl-xL sequestration can occur in a p53-dependent manner.[21] These data indicate the need for further study of p53 activation in hT17M *Rho* retinas.

The mechanisms by which pro-apoptotic activation occurs include posttranslational alterations, such as phosphorylation (Bad and Bik/Nbk) or proteolytic cleavage (the truncation of Bid by caspase-8).[17] Therefore, we next asked the question: "Is there a direct link between overproduction of these proteins and their activation"? Based on our results, there does appear to be a connection. Our analysis of the retinal mitochondrial fraction shows a 55% increase in the release of AIF1 from the hT17M *Rho* mitochondria, indicating that the mitochondria permeability transition pore (MPTP) already exists by P21. This result implies that the over-expression of BH3-only proteins correlates with an increase in their post-translational modification.

Pro-survival markers, such as Akt signaling and Bcl2 over-expression, are present in hT17M *Rho* retinas. Akt signaling controls the dissociation of Bad protein from the Bcl-2/Bcl-X complex and the loss of its pro-apoptotic function.[22] In our experiments, *Bad* gene expression was found not to be elevated in hT17M *Rho* retinas, and it is possible that the Akt-controlled posttranscriptional phosphorylation of Bad affects its transcriptional level. Another signaling molecule, the anti-apoptotic gene *Bcl-2*, is up-regulated in hT17M *Rho* retinas after P12, at which point the expression of the *Chop* gene already is increased. The *Bcl-2* gene is known to be a transcriptional control target of the CHOP transcriptional factor.[23] Therefore, after P15, when *Chop* expression decreases, *Bcl2* gene expression increases. Both pro-survival pathways are up-regulated in hT17M *Rho* retinas in an attempt to balance the expression of pro-apoptotic Bcl2 proteins and restore homeostasis in hT17M *Rho* photoreceptors. Simultaneous activation of pro- and anti-apoptotic pathways in our experiment, however, could be accounted for by different dynamics of degeneration in different retinal cell types. For example, while rod photoreceptors already are undergoing suicide by apoptosis, neighboring cells, such as cone photoreceptors and retinal ganglia cells, still are struggling to prevent apoptosis.

Finally, we found that ER stress and mitochondria-associated apoptosis lead to the final demise of photoreceptors (Figs. 6, 7A). Both caspase-3 and caspase-12 are up-regulated. However, caspase-3 is up-regulated earlier than caspase-12, suggesting that other cellular pathways lead to the activation of the executioner caspase. These findings are consistent with the rate of adRP progression in transgenic retinas measured by OCT (Fig. 7C). At 1 month, transgenic mice already have lost 50% of their photoreceptors, resulting in the downregulation of the transcriptional factors *Nrl* and *Crx* starting as early as P15 and P18. These changes apparently are responsible for decrease in the level of Rho protein in hT17M *Rho* retina.

To our knowledge, for the first time, we demonstrated that the ER stress response is involved in retinal degeneration in hT17M *Rho* retinas, and correlates strongly with the up-regulation of autophagy markers and the activation of mitochondrial signaling via the up-regulation of pro-apoptotic *Bcl2* genes. The results of our experiments allow us to identify the following genes that could be potential therapeutic targets for adRP treatment: *Atg5*, *Atg7*, *Bax*, *Bid*, *Bik,* and *Noxa*.

Acknowledgments

The Riken Bioresource Center, Tokyo, Japan provided the ERAI mice.

References

1. Dryja TP, McGee TL, Hahn LB, et al. Mutations within the rhodopsin gene in patients with autosomal dominant retinitis pigmentosa. *N Engl J Med*. 1990;323:1302–1307.
2. Krebs MP, Holden DC, Joshi P, Clark CL III, Lee AH, Kaushal, S. Molecular mechanisms of rhodopsin retinitis pigmentosa and the efficacy of pharmacological rescue. *J Mol Biol*. 2010;395:1063–1078.
3. Tam BM, Moritz OL. The role of rhodopsin glycosylation in protein folding, trafficking, and light-sensitive retinal degeneration. *J Neurosci*. 2009;29:15145–15154.
4. Kaushal S, Khorana HG. Structure and function in rhodopsin. 7. Point mutations associated with autosomal dominant retinitis pigmentosa. *Biochemistry*. 1994;33:6121–6128.
5. Li T, Sandberg MA, Pawlyk BS, et al. Effect of vitamin A supplementation on rhodopsin mutants threonine-17 $\geq$ methionine and proline-347 $\geq$ serine in transgenic mice and in cell cultures. *Proc Natl Acad Sci U S A*. 1998;95:11933–11938.
6. Chen Y-F, Wang I-J, Lin LL, Chen MS. Examining rhodopsin retention in endoplasmic reticulum and intracellular localization in vitro and in vivo by using truncated rhodopsin fragments. *J Cell Biochem*. 2011;112:520–530.

7. Lin JH, Li H, Zhang Y, Ron D, Walter P. Divergent effects of PERK and IRE1 signaling on cell viability. *PLoS One*. 2009;4: e4170.
8. Gorbatyuk MS, Knox T, LaVail MM, et al. Restoration of visual function in P23H rhodopsin transgenic rats by gene delivery of BiP/Grp78. *Proc Natl Acad Sci U S A*. 2010;107:5961–5966.
9. Duricka D, Brown RL, Varnum MD. Defective trafficking of cone photoreceptor CNG channels induces the unfolded protein response and ER stress-dependent cell death. *Biochem J*. 2011;441:685–696.
10. Lin JH, Li H, Yasumura D, et al. IRE1 signaling affects cell fate during the unfolded protein response. *Science*. 2007;318:944–949.
11. Griciuc A, Aron L, Ueffing M. ER stress in retinal degeneration: a target for rational therapy? *Trends Mol Med*. 2011;17:442–451.
12. Iwawaki T, Akai R, Kohno K, Miura M. A transgenic mouse model for monitoring endoplasmic reticulum stress. *Nat Med*. 2004;10:98–102.
13. Krebs MP, White DA, Kaushal S. Biphasic photoreceptor degeneration induced by light in a T17M rhodopsin mouse model of cone bystander damage. *Invest Ophthalmol Vis Sci*. 2009;50:2956–2965.
14. Mao H, James T Jr, Schwein A, et al. AAV delivery of wild-type rhodopsin preserves retinal function in a mouse model of autosomal dominant retinitis pigmentosa. *Hum Gene Ther*. 2011;22:567–575.
15. Gorbatyuk M, Justilien V, Liu J, Hauswirth WW, Lewin AS. Preservation of photoreceptor morphology and function in P23H rats using an allele independent ribozyme. *Exp Eye Res*. 2007;84:44–52.
16. Rzymski T, Milani M, Pike L, et al. Regulation of autophagy by ATF4 in response to severe hypoxia. *Oncogene*. 2010;29: 4424–4435.
17. Szegezdi E, Macdonald DC., Ni Chonghaile T, Gupta S, Samali A. Bcl-2 family on guard at the ER. *Am J Physiol Cell Physiol*. 2009;296:C941–953.
18. Zhang F, Hamanaka RB, Bobrovnikova-Marjon E, et al. Ribosomal stress couples the unfolded protein response to p53-dependent cell cycle arrest. *J Biol Chem*. 2006;281: 30036–30045.
19. Basu A, Haldar S. The relationship between BcI2, Bax and p53: consequences for cell cycle progression and cell death. *Mol Hum Reprod*. 1998;4:1099–1109.
20. Hur J, Bell DW, Dean KL, et al. Regulation of expression of BIK proapoptotic protein in human breast cancer cells: p53-dependent induction of BIK mRNA by fulvestrant and proteasomal degradation of BIK protein. *Cancer Res*. 2006; 66:10153–10161.
21. Song G, Wang W, Hu T. p53 Facilitates BH3-only BID nuclear export to induce apoptosis in the irrepairable DNA damage response. *Med Hypotheses*. 2011;77:850–852.
22. Datta SR, Dudek H, Tao X, et al. Akt phosphorylation of BAD couples survival signals to the cell-intrinsic death machinery. *Cell*. 1997;91:231–241.
23. Chiribau CB, Gaccioli F, Huang CC, Yuan CL, Hatzoglou M. Molecular symbiosis of CHOP and C/EBP beta isoform LIP contributes to endoplasmic reticulum stress-induced apoptosis. *Mol Cell Biol*. 2010;30:3722–3731.